

**Figure S1A**

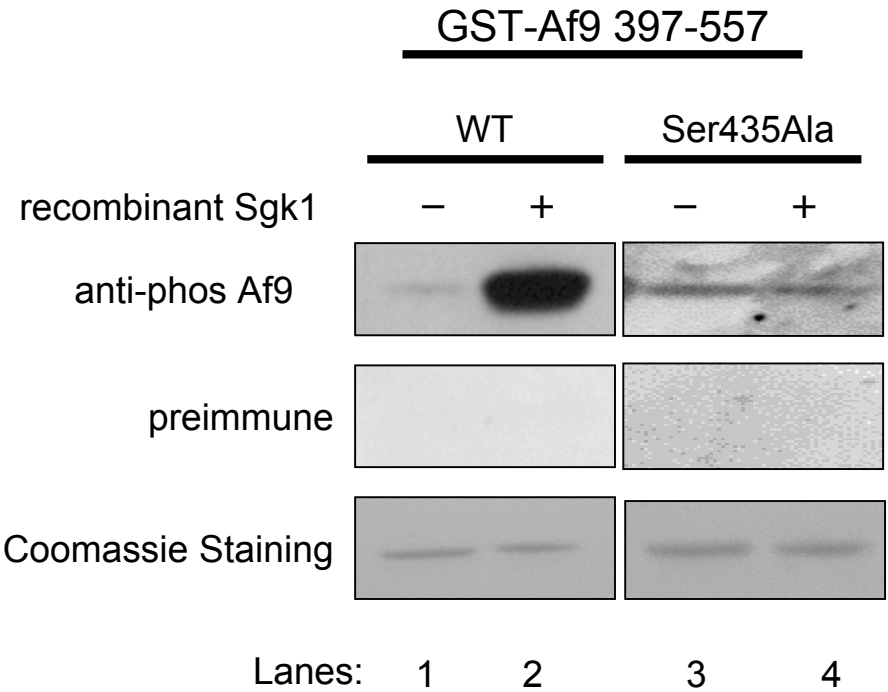


Figure S1B

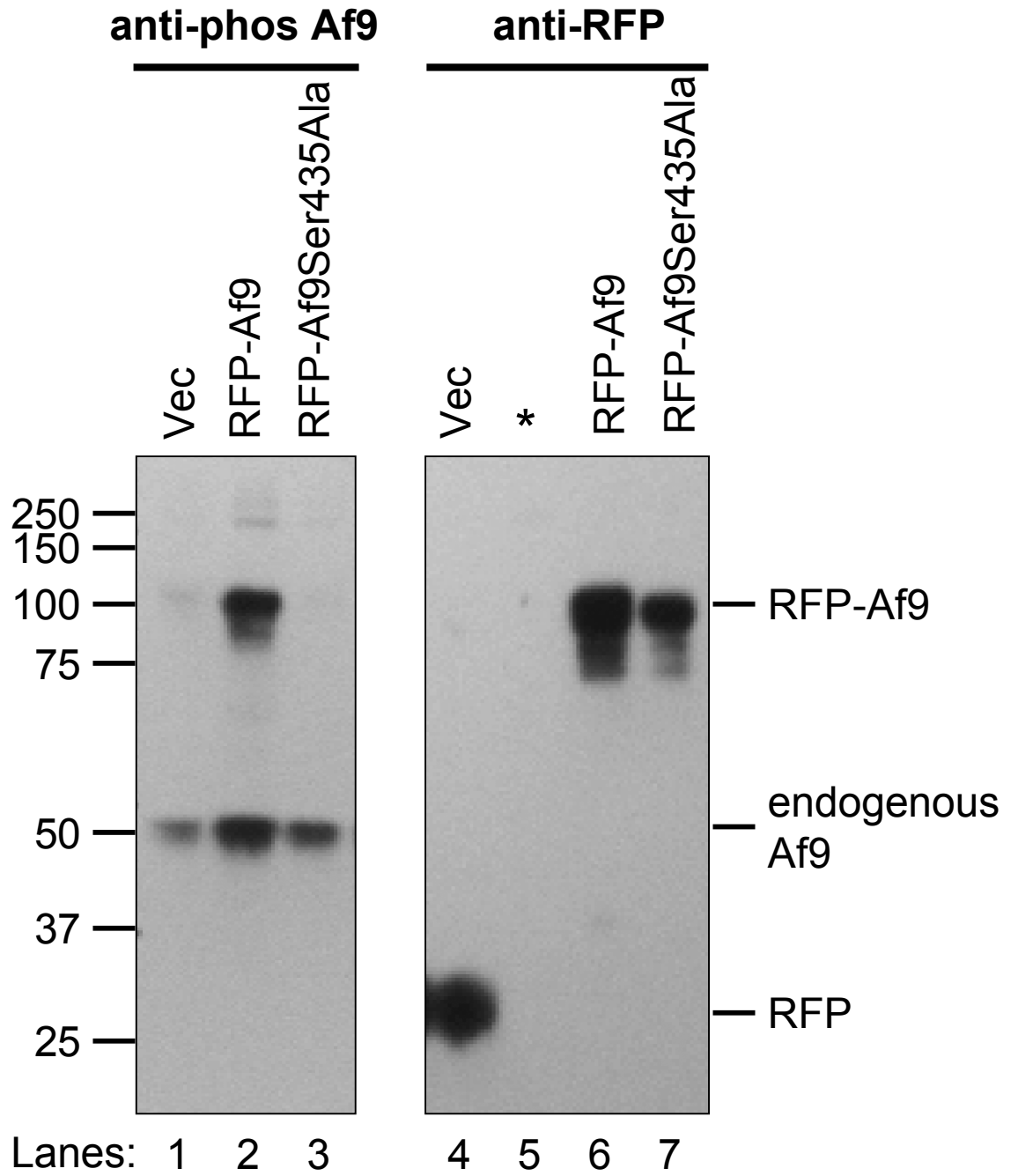


Figure S2A

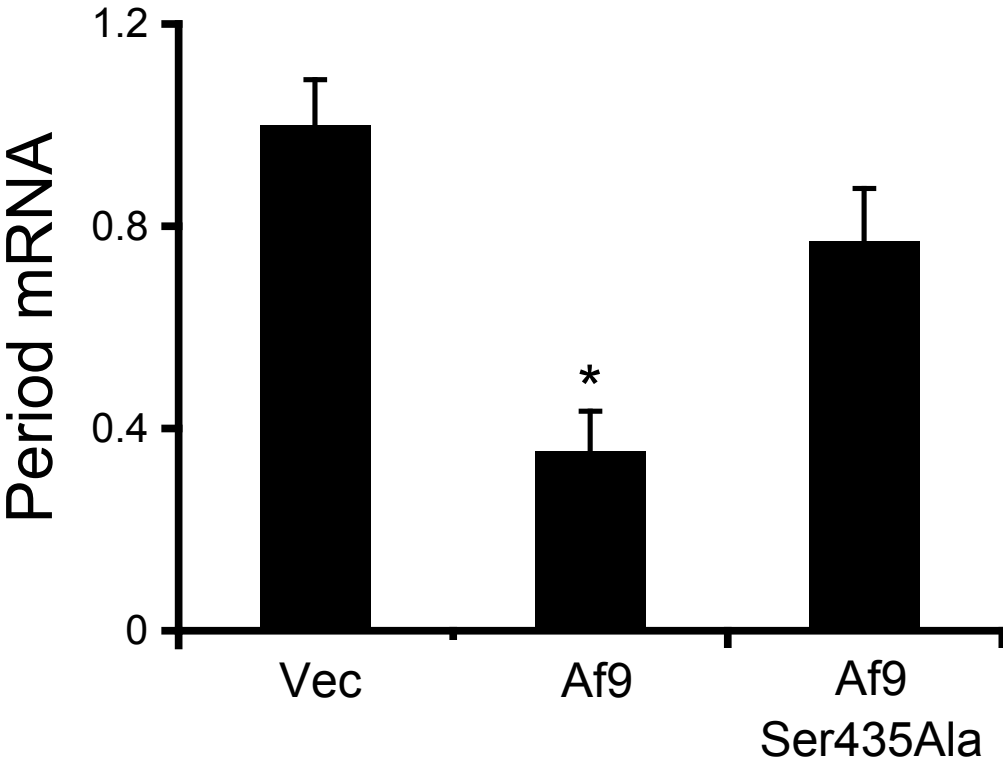


Figure S2B

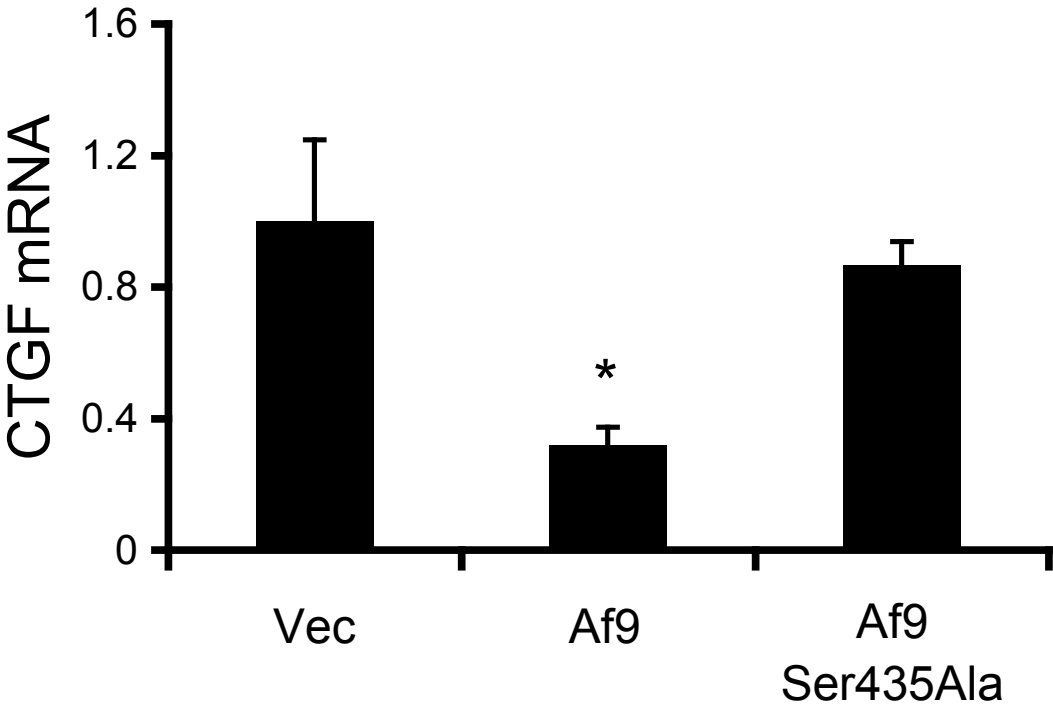
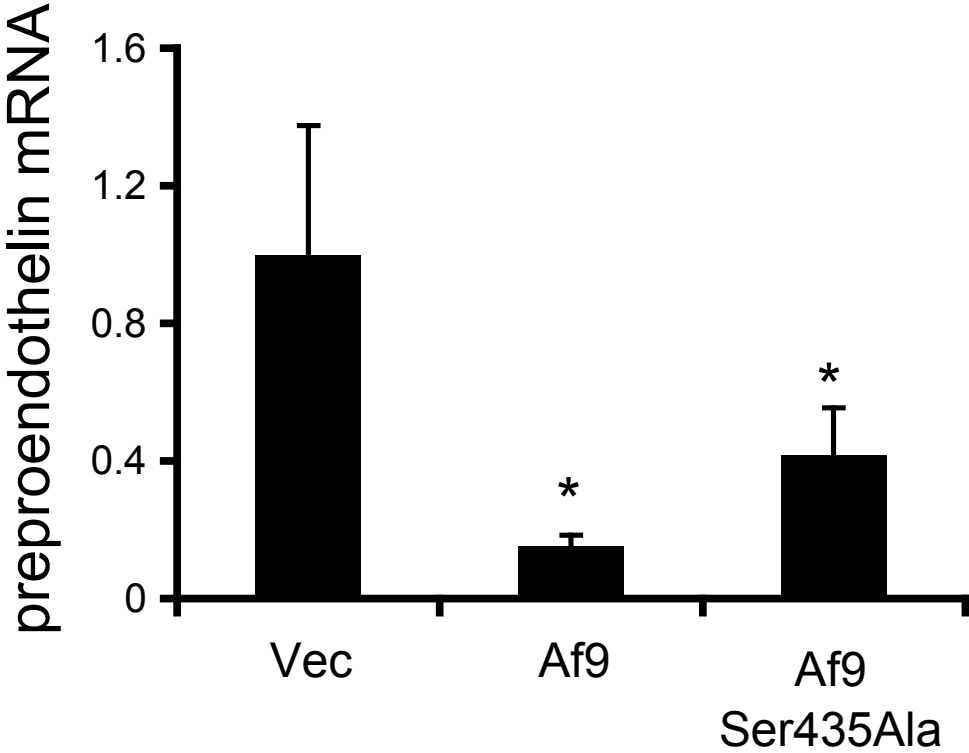


Figure S2C



## SUPPLEMENTAL DATA

### LEGENDS TO SUPPLEMENTAL FIGURES

#### **Fig. S1. Characterization of an anti-Af9 antibody specific for phosphorylated Ser435.**

Characterization of the anti-phospho-Af9 antibody (anti-phos Af9) using GST-Af9 fusions. As in Fig. 1C, GST-Af9 fusions containing aa 397-557 with or without S435A mutation were subjected to in vitro phosphorylation as indicated, and analyzed by immunoblotting probed with the anti-phospho-Af9 antibody (upper) or preimmune serum (middle). Coomassie staining of identical gels showing approximate equal loading of the fusions (bottom). n=2. **B.** Characterization of the anti-phospho-Af9 antibody specific for phosphorylated S435 using RFP-Af9 fusions. Whole cell lysates of mIMCD3 cells transiently transfected with pDsRed-monomer (Vec) or its derivatives encoding RFP-Af9 or RFP-Af9 Ser435Ala (RFP-Af9 Mut) were analyzed by immunoblotting with the antibodies indicated. RFP-Af9 apparently migrated at ~110 kd, slower than its expected size of ~90kd. \*: blank lane with no samples were loaded. n=2.

#### **Figure S2. A-C. Real-time RT-qPCR showing that the Ser435Ala mutation largely abolishes AF9 overexpression-dependent repression of other aldosterone target genes in mIMCD3 cells.**

Total RNAs from mIMCD3 cells transiently transfected with pCMV500 (Vec), pFLAG-Af9 (Af9), or pFLAG-Af9 Ser435Ala were analyzed by real-time RT-qPCR to determine the mRNA levels of the genes indicated and normalized to that of GAPDH from the same sample. GAPDH levels were invariant under the different conditions. \*: P<0.05 versus Vec. n=3.